



Continuous fixed-bed adsorption of Congo red dye by dual adsorbent (*Neurospora crassa* dead fungal biomass and wheat bran): experimental and theoretical breakthrough curves, immobilization and reusability studies

P. Vairavel^a, V. Ramachandra Murty^{b,*}

^aDepartment of Chemical Engineering, Manipal Institute of Technology, Manipal Academy of Higher Education, Manipal, Karnataka, India, Tel. +919036270978, email: pvairavel@gmail.com

^bDepartment of Biotechnology, Manipal Institute of Technology, Manipal Academy of Higher Education, Manipal, Karnataka, India, Tel. +91 9448529691, email: murty.vytla@manipal.edu

Received 3 May 2017; Accepted 24 September 2017

ABSTRACT

A continuous study in a fixed-bed adsorption column was carried out by using dead fungal biomass of *Neurospora crassa* with wheat bran as a dual adsorbent for the removal of Congo red (CR) from aqueous solutions. Adsorption experiments were conducted at 303 K and at pH 6. The effect of operating parameters such as bed height (2–4 cm), flow rate (1–5 mL min⁻¹), and influent dye concentrations (10–50 mg L⁻¹) on the breakthrough characteristics of the CR adsorption system were determined using free dual adsorbent. Data confirmed that the total amount of adsorbed dye decreased with increasing flow rate and increased with increasing bed height and inlet adsorbate concentration. The highest column adsorption capacity of 5.71 mg g⁻¹ was obtained using 50 mg L⁻¹ inlet adsorbate concentration, 2 cm bed height, and 1 mL min⁻¹ flow rate. The dual adsorbent was immobilized in various polymeric matrices such as calcium alginate, polyvinyl alcohol, polysulfone and sodium silicate. Batch experiments were conducted to select a suitable matrix for immobilization of the dual adsorbent. The maximum percentage of CR adsorption (84.72%) occurred using the polymeric matrix sodium silicate. Desorption studies were conducted in batch mode to desorb the CR dye from free and immobilized dual adsorbents using the desorbing agent methanol. Reusability studies of free and immobilized dual adsorbents for the adsorption of CR dye were carried out in three cycles in continuous mode. The equilibrium dye uptake and percentage adsorption of the regenerated free and immobilized dual adsorbents were decreased significantly after the first cycle. The percentage adsorption and equilibrium dye uptake using immobilized dual adsorbent in all three runs were lower than when free dual adsorbent was used. The percentages of dye adsorption were 57.75% and 41.70%; equilibrium dye uptakes were 0.696 mg g⁻¹ and 0.35 mg g⁻¹ in the third run of operation with free and immobilized dual adsorbent, respectively. Various mathematical models such as Adams-Bohart, bed depth service time (BDST), Thomas and Yoon-Nelson models were applied to column experimental data to predict the breakthrough curve and to evaluate the column capacity and kinetic constants of the models. The results fitted well to the experimental values in Thomas and Yoon-Nelson models with coefficients of correlation $R^2 \geq 0.967$ at different operating conditions. The adsorption of solute from textile industrial CR dye effluent was carried out in column studies separately, using free and immobilized dual adsorbents. The percentages of solute adsorption were 82.18% and 67.34%; equilibrium solute uptakes were 10.79 mg g⁻¹ and 8.26 mg g⁻¹ with free and immobilized dual adsorbent, respectively. We concluded that the dead fungal biomass of *Neurospora crassa* with wheat bran were shown to be suitable dual adsorbent for adsorption of CR using fixed-bed adsorption column and it can be used effectively in wastewater treatment.

Keywords: Congo red dye; *Neurospora crassa* dead fungal biomass; Wheat bran; Fixed-bed column; Mathematical models; Immobilization

*Corresponding author.

1. Introduction

Nowadays, one of the key environmental problems facing humanity is the increasing worldwide contamination of freshwater systems with thousands of industrial chemical compounds. The intensive development of industry is accompanied by a decrease of environmental quality. Although industrial development involves implementation of environmentally accepted processes, large quantities of industrial wastewaters are discharged into the environment [1]. Dyes are widely used in many industries such as textiles, rubber, cosmetics, paper, carpet, printing, leather, etc. The release of dye effluent by various industries imparts color to the natural receiving water bodies, making them unacceptable for public consumption [2]. Currently more than 1×10^5 dyes are commercially available having various applications with a global annual production in excess of 7×10^5 million tons [3]. Worldwide, the total dye consumption of the textile industry is in excess of 10^7 kg year⁻¹ [4]. However, approximately 1 million kg of textile dyes are discharged into industrial effluents every year [5]. On the other hand around 10–15% dyes were released into the environment during their manufacturing and usage [6]. Generally, color is visible in the effluents from textile-dyeing processes when the dye concentration is greater than 1 mg L⁻¹ and at an average concentration of 300 mg L⁻¹ [7]. Congo red (disodium salt of benzidinediazo-bis-1-naphthylamine-4-sulfonic acid) is a polar anionic diazo dye prepared by coupling tetra-azotised benzidine with two molecules of naphthionic acid. It has a strong affinity for cellulose fibers and is used in textile industries (dyeing cottons, and wools) [8]. It has been known to cause an allergic reaction and to be metabolized to benzidine, a human carcinogen [9]. Even a low concentration of azo dye causes various harmful effects such as difficulties in breathing, vomiting, diarrhea, nausea, abdominal and chest pain, severe headache, etc. [8]. Furthermore, dyes can significantly affect photosynthetic activity in aquatic systems. Dyes are highly toxic, carcinogenic and usually constitute health hazards [10]. The effluents must be treated to bring down the concentration of dyes present in it to permissible and bearable limit [11,12]. Hence, the removal of CR is also of great environmental importance.

Most dye effluents can be treated by conventional treatment methods, such as coagulation, membrane filtration, ion exchange, photochemical oxidation, ozonation, Fenton process, electrochemical oxidation, and sonication [11,12]. However, these technologies have several disadvantages such as high capital and operating cost, complexity of the treatment processes, sludge disposable problem, and the need of chemicals, which may in turn pollute the water [13,14]. Due to these limitations, there is vital need for a more environmentally benign and cost effective method. Furthermore, these methods are cannot be used effectively to treat the wide range of dye wastewaters [15]. Furthermore, these methods are cannot be used effectively to treat the wide range of dye wastewaters. Liquid phase adsorption is widely used in the removal of toxic pollutants from effluent since proper design of the adsorption process will produce a high-quality treated effluent. This process provides an attractive alternative for the treatment of contaminated waters, especially if the adsorbent is inexpensive [16]. Adsorption has been found to be superior to other techniques for water re-use in terms of initial cost, flexibility

and simplicity of design, ease of operation and insensitivity to toxic pollutants. Additionally, this process is more eco-friendly because it does not result in the formation of harmful substances [11,14]. Adsorption on commercial activated carbon has been found to be an effective process because of its excellent adsorption ability, but it is highly expensive and regeneration of spent activated carbon is relatively difficult [17]. To reduce the cost of the treatment process, attention has been focused on the development of low-cost, easily available and highly effective adsorbents [18]. Various low-cost adsorbents from agricultural by-products have been used to remove color from aqueous solutions. These adsorbents include wheat bran [19], rice husks [20], orange peels [21], papaya seeds [22], neem leaves [23], garlic peels [24] and wheat husks [25].

In biological treatments, microbial decolorization of dye can be classified into two kinds according to their life state: For living cells, the major mechanism is biodegradation because they can produce lignin modifying enzymes, laccase, manganese peroxidase (MnP) and lignin peroxidase (LiP) to biodegrade/biotransform the synthetic dyes. For dead cells, the mechanism is biosorption, which involves physico-chemical interaction between adsorbate and adsorbent [26,27]. Various types of dead fungal biomass such as *Neurospora crassa* [28], *Rhizopus stolonifera* [29], and *Agaricus bisporus* [30], among others, can be used to decolorize dye wastewater.

The use of adsorbent for large-scale process utilization (column applications) has some problems such as small particle size, low mechanical strength and poor rigidity. The separation of adsorbent after adsorption becomes difficult and results in loss of adsorbent after regeneration. These problems may be rectified by immobilizing the adsorbent using supporting materials such as a polymeric matrix [31]. Immobilization may improve the mechanical strength, resistance to different chemical compounds and ease of regeneration and reuse [32]. In practice, the continuous fixed-bed adsorption operation is a more effective process for numerous adsorption/desorption cycles in large-scale treatment of wastewater [33]. The column studies are essential to obtain the parameters required for the design of fixed-bed adsorbers [17]. The concentration gradient is the driving force for adsorption and permits more efficient saturation of adsorbent. A large volume of effluent can be treated continuously using a fixed quantity of adsorbent in the column and results in a better quality of the effluent [33]. The column becomes saturated as the available binding sites are occupied by the target adsorbate molecules [34]. The adsorbent can be regenerated by using an appropriate desorbing agent for its reuse [33]. The advantages of the fixed-bed column over the batch mode of operation are minimum damage due to particle attrition and easy scale-up [33,35]. The potential of using dead biomass with wheat bran as effective dual adsorbent to remove azo dyes has not been explored. The dual adsorbent had better adsorption efficiency in the removal of color from dye wastewater when compared to the individual adsorbents and the process with dual adsorbent is rapid [36,37]. The literature survey indicates that adsorption studies of toxic compounds in this area are limited. Biosorption of selected toxic organics with a few types of bacterial or fungal biomass and the use of

agricultural by-products as a low-cost adsorbent of dye molecules have been investigated. Therefore, the present study was focused on dual adsorbent consisting of dead fungal biomass of *Neurospora crassa* and wheat bran for the adsorption of CR dye from a synthetic effluent. Fixed-bed column studies were performed on CR dye adsorption using free and immobilized dual adsorbents to determine the experimental breakthrough curve (BTC). *Neurospora crassa* is a filamentous non-pathogenic ascomycete fungus [28,38]. Wheat bran is the outer shell of wheat grain, and a by-product of the wheat milling operation; furthermore, wheat bran is an economically viable and most readily available natural material in India.

2. Materials and methods

2.1. Preparation of wheat bran and *Neurospora crassa* dead biomass dual adsorbent

Wheat bran was procured from M/s Ganesh flour-mill industries, Kolkata, India. It was washed with distilled water to remove soluble impurities. Then the bran was dried in a hot-air oven at the temperature of 378 K for 24 h, ground and screened to obtain particles <100 μm in size [19]. The filamentous fungus *Neurospora crassa* (MTCC 1852) was obtained from the Institute of Microbial Technology, Chandigarh, India and was stored at 277 K. In total 100 mL of potato dextrose broth medium was inoculated with the live fungal culture in Erlenmeyer flasks under sterile conditions. The fungi were allowed to grow for one week in an incubator shaker rotated at a speed of 120 rpm at 298 K [38]. After sufficient growth, the live fungal biomass was filtered and washed thoroughly with distilled water. Furthermore, the dead biomass was prepared by keeping the live biomass in an oven for 24 h on Petri plates at 333 K and powdered using a mortar and pestle. The material was screened to obtain particles <100 μm in size. The dual adsorbent is the mixture of dead fungal biomass and wheat bran. The optimum amounts of dead biomass and wheat bran were mixed in the proportion of 3:10 (based on weight) which means that 15 g of dead biomass was mixed with 50 g of wheat bran to prepare dead biomass-wheat bran dual adsorbent (DB-WB). The optimum concentration of dead biomass (3 g L⁻¹) and wheat bran (10 g L⁻¹) were added to the dye solution gives the maximum percentage of CR decolorization in previous batch studies. The optimum amounts of each adsorbents were obtained from factorial experimental design (CCD). The detailed procedure for evaluation of optimized values of individual adsorbents was given elsewhere [36]. No other physical or chemical treatment was used prior to the adsorption experiments.

2.2. Characterization of dead biomass-wheat bran dual adsorbent

The prepared dual adsorbent was characterized by particle size, surface area, pore volume, Fourier Transform Infrared Spectroscopy (FT-IR), and Scanning Electron Microscopy (SEM) analysis. The characterization of DB-WB dual adsorbent was given elsewhere [36].

2.3. Chemicals required

An anionic dye Congo red (Dye content $\geq 35\%$, Molecular formula = C₃₂H₂₂N₆Na₂O₆S₂, Molecular weight = 696.66, λ_{max} = 498 nm) supplied by Sigma Aldrich, India was used in the study. The dye was of analytical reagent grade and of 99.8% purity. The analytical grade of potato dextrose agar and potato dextrose broth were obtained from Himedia, India. All other chemicals such as sodium hydroxide, hydrochloric acid, sodium alginate, calcium chloride, polyvinyl alcohol, polysulfone, dimethylformamide, sodium silicate, sulfuric acid, acetic acid, and methanol used were of analytical grade (Merck, India).

2.4. Preparation of CR dye stock solution

The required amount of CR dye powder was dissolved in distilled water to prepare a 1000 mg L⁻¹ stock solution. This stock solution was further diluted with pH adjusted distilled water by adding 0.1 N HCl or 0.1 N NaOH to obtain the required concentration range. After dilution (adjusting the pH), the final pH of the dye solution was measured as 6 and further adsorption experiments were carried out at pH 6, because the red color remained stable in the pH range of 6–14. Batch studies results showed that maximum adsorption of CR was observed at pH 6 [36]. At pH 6, a significant electrostatic attraction exists between the positively charged surfaces of dual adsorbent and anionic CR dye molecules. Moreover, CR dye color becomes unstable if the solution pH decreased less than 6 because of the formation of protonated species, which may lead to a change in the structure of the dye. The CR dye in aqueous solution was black in color at acidic pH (< 5), due to the formation of a quinonoid structure [39].

2.5. Analytical measurements

The pH of the dye solution was observed by a digital pH-meter (Systronics 335). After adsorption, the samples were centrifuged in a cooling centrifuge (Remi CPR-24 Plus). A double-beam UV/visible spectrophotometer (Shimadzu UV-1800) operating at the wavelength (λ_{max}) of 498 nm was used to determine the unknown residual concentration of CR dye solution.

2.6. Column experiments with synthetic dye wastewater using free DB-WB dual adsorbent

To study the dynamic adsorption behavior, continuous flow fixed-bed adsorption experiments were conducted in a glass column of 2.1-cm inner diameter and 39-cm height. A schematic diagram of the fixed-bed column is given in Fig. 1. A rubber cork of 1.5 cm was provided at the top and bottom of the column to support the inlet and outlet pipes. The column was packed with 2 cm of glass wool followed by glass beads (1.5 mm in diameter) both at the top and bottom [40]. The dead biomass-wheat bran dual adsorbent was added to the column with varying quantities as 2.97, 4.45 and 5.94 g to produce various bed heights of 2, 3 and 4 cm respectively. An aqueous CR dye solution of known concentration at pH 6 was pumped in an upward direction through the column by a peristaltic pump at the

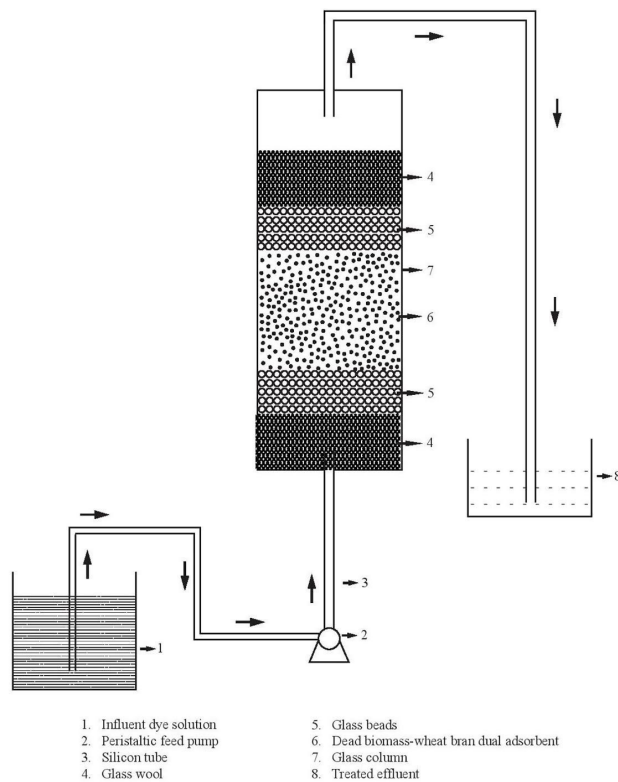


Fig. 1. Schematic diagram of the fixed-bed adsorption column.

required flow rate. The treated dye solution was collected at uniform time intervals from the top of the column with the flow rate the same as the feed stream. The concentration of unadsorbed dye solution was noted using a UV/visible spectrophotometer. The experiments were continued until the concentration of treated solutions reached the feed concentration of adsorbate [41]. Fixed-bed column studies were performed to study the effect of bed height, flow rate and inlet adsorbate concentration on CR dye adsorption.

2.7. Mathematical description of adsorption in a continuous fixed-bed column

The performance of the fixed-bed column was analyzed through the concept of BTC. The breakthrough point (BP) is the point at which the concentration of solute in the effluent starts to rise appreciably. The breakthrough point time (t_B) and shape of the BTC are important parameters to design the large-scale adsorption column. BTC is the ratio of effluent adsorbate concentration to inlet adsorbate concentration (C_t/C_o) as a function of time or volume of the effluent. The effluent volume (V_{eff}) can be calculated as follows [42]:

$$V_{eff} = Q t_{total} \quad (1)$$

where Q and t_{total} are the volumetric flow rate (mL min^{-1}) and total flow time (min). The total quantity of solute adsorbed (m_{ad}) in the column is obtained by the area above BTC multiplied by the flow rate and initial adsorbate concentration. It is represented as [43].

$$m_{ad} = \left[\int_0^{t_E} \left(1 - \frac{C_t}{C_o} \right) dt \right] C_o Q \quad (2)$$

where t_E is the bed exhaustion time (min), which is the time at which the pollutant concentration in the effluent reached 99.5% of the initial feed concentration. The total amount of dye sent through the column (m_{total}) was calculated by the following equation [42]:

$$m_{total} = \frac{C_o Q t_{total}}{1000} \quad (3)$$

The total percentage dye adsorption in the column is described as follows [40]:

$$\text{Total dye removal (\%)} = \frac{m_{ad}}{m_{total}} \times 100 \quad (4)$$

Equilibrium dye uptake in the column was calculated from Eq. (5) [41].

$$q_e = \frac{m_{ad}}{W} \quad (5)$$

where W is the mass of dry dual adsorbent (g).

2.8. Modeling of column experimental data

The various mathematical model equations such as Adams-Bohart, bed depth service time (BDST), Thomas and Yoon-Nelson models were used for the design of the column adsorption process and to scale it up for industrial applications. The linear regression analysis is used to determine the kinetic constants [44].

2.8.1. Adams-Bohart Model

The Adams-Bohart model is used for the description of the initial part of the BTC. The model assumes that the rate of adsorption is proportional to the residual capacity of adsorbent and concentration of the adsorbing species, given by the following linear equation [41]:

$$\ln \left(\frac{C_t}{C_o} \right) = K_{AB} C_o t - \frac{K_{AB} N_o Z}{U_o} \quad (6)$$

where C_o is the initial adsorbate concentration (mg L^{-1}), C_t is the effluent concentration of adsorbate at time t (mg L^{-1}), t is the flow time (min), K_{AB} is the kinetic constant ($\text{L mg}^{-1} \text{min}^{-1}$), N_o is the maximum saturation concentration (mg L^{-1}), Z is the bed height (cm), and U_o is the superficial velocity (cm min^{-1}). From this equation, the characteristic operational parameters K_{AB} and N_o can be determined from the slope and intercept of the plot of $\ln \left(\frac{C_t}{C_o} \right)$ vs. t .

2.8.2. Bed depth service time (BDST) model

BDST is a simple model for predicting relationship between bed depth, Z , and service time, t , in terms of pro-

cess concentrations and adsorption parameters. It is based on the assumption that the rate of adsorption is controlled by the surface reaction between adsorbate and the unused capacity of the adsorbent. In the BDST model, movement of the adsorption wave front through the adsorption bed, that is, the service time t of a column, is given by the following linear equation [45]:

$$t = \left(\frac{N_o Z}{C_o U_o} \right) - \left(\frac{1}{C_o K} \right) \ln \left(\frac{C_o}{C_t} - 1 \right) \quad (7)$$

where K is the adsorption rate constant ($\text{L mg}^{-1} \text{min}^{-1}$). The linear plot of t vs. $\ln \left(\frac{C_o}{C_t} - 1 \right)$ permits the determination of N_o and K from the intercept and slope of the plot.

2.8.3. Thomas model

The Thomas model is used to analyze the column performance for adsorption of CR dye. The linear expression of this model equation is given by [33]:

$$\ln \left(\frac{C_o}{C_t} - 1 \right) = \frac{K_{Th} q_{oTh} W}{Q} - \frac{K_{Th} C_o V_{eff}}{Q} \quad (8)$$

where K_{Th} is the Thomas rate constant ($\text{L min}^{-1} \text{mg}^{-1}$) and q_{oTh} is the maximum solid phase concentration of the solute (mg g^{-1}). The plot of $\ln \left(\frac{C_o}{C_t} - 1 \right)$ vs. V_{eff} yields a straight line for which the slope K_{Th} and intercept q_{oTh} are estimated.

2.8.4. Yoon-Nelson model

The Yoon-Nelson model is based on the assumption that the rate of decrease in the probability of adsorption for each adsorbate molecule is proportional to the probability of adsorbate adsorption and the probability of adsorbate breakthrough on the adsorbent. A linear form of this model equation is expressed as follows [46]:

$$\ln \left(\frac{C_t}{C_o - C_t} \right) = k_{YN} t - \tau k_{YN} \quad (9)$$

where k_{YN} is the Yoon-Nelson rate constant (min^{-1}) and τ is the time required for 50% solute breakthrough (min). The values of k_{YN} and τ are determined from the slope and intercept, respectively, of the linear plot of $\ln \left(\frac{C_t}{C_o - C_t} \right)$ vs. sampling time t . Hence, the adsorption bed should be completely saturated at $t = 2\tau$. Therefore, the amount of dye adsorbed in the fixed-bed is half of the total dye entering the adsorption bed within a 2τ period. The adsorption capacity of the column in this model (q_{oYN}) can be obtained as [33]:

$$q_{oYN} = \frac{C_o Q \tau}{1000W} \quad (10)$$

2.9. Immobilization of the DB-WB dual adsorbent for CR dye adsorption

The various matrices used for the immobilization of dead biomass-wheat bran dual adsorbent are calcium alginate gel, polyvinyl alcohol, polysulfone and sodium silicate [32,47].

2.9.1. Immobilization of the dead biomass-wheat bran dual adsorbent in calcium alginate

A slurry of 2% (w/v) sodium alginate was prepared in hot distilled water at 333 K for 1 h, resulting in a transparent and viscous solution [48,49]. After cooling, varying quantities (2–10% w/v) of dual adsorbent powder were added and stirred for 30 min [32]. For polymerization and preparation of beads, the alginate-dual adsorbent slurry was extruded drop by drop into a cold, sterile 0.05 M CaCl_2 solution with the help of a sterile 12 mL syringe (2 mm, ID) [32,50]. The water-soluble sodium alginate was converted into water-insoluble calcium alginate entrapped on dual adsorbent beads on treatment with calcium chloride [48]. The beads were hardened by re-suspending them into a fresh cold 0.05 M calcium chloride solution for 24 h with gentle agitation [51].

2.9.2. Immobilization of the dead biomass-wheat bran dual adsorbent in polyvinyl alcohol

A polyvinyl alcohol-sodium alginate slurry was prepared in hot distilled water at 333 K for 1 h in a beaker. The weight ratio between polyvinyl alcohol and sodium alginate was kept at 2:1 which means that 2 g of polyvinyl alcohol was mixed with 1 g of sodium alginate in 100 mL hot distilled water. The various quantities of dual adsorbent powder (2–10% (w/v)) were added to the slurry and the mixtures were stirred for 30 min. Beads were prepared as mentioned above in section 2.9.1 for polyvinyl alcohol-alginate-dual adsorbent slurry in 4% (w/v) cold CaCl_2 solution. The beads were hardened by re-suspending them into a fresh cold 4% (w/v) calcium chloride solution for 6 h with gentle agitation. After 6 h of stabilization, the beads were subjected to three cycles of freezing at $< 275 \text{ K}$ and thawing at 303 K to get spherical beads [32].

2.9.3. Immobilization of the dead biomass-wheat bran dual adsorbent in polysulfone

A 10% (w/v) solution of polysulfone was prepared in dimethylformamide. Required quantities of the dual adsorbent (2–10% (w/v)) were mixed with the polysulfone slurry. Beads were prepared by following the above procedure as mentioned in section 2.9.1. The slurry was polymerized in distilled water. The immobilized beads were cured for 16 h in distilled water [32].

The various immobilized beads were washed with distilled water and kept in an oven at 323 K for 24 h [48]. Finally, the resultant bead diameter was experimentally estimated and found to be 2.4 mm.

2.9.4. Immobilization of the dead biomass-wheat bran dual adsorbent in sodium silicate

A 6% (w/v) sodium silicate solution was prepared with distilled water in an Erlenmeyer flask. The sodium silicate solution was added dropwise into 15 mL of 5% (v/v) sulfuric acid until the pH reached 2. The various quantities of dual adsorbent powder (1–10% (w/v)) were dissolved in 2% (v/v) acetic acid. Then, 50 mL of this adsorbent dissolved solution was added drop by drop to the silicate solution and the mixture was rotated for 15 min. The polymeric gel was made by addition of sodium silicate solution to reach pH 7. The resultant gel was purified using distilled water to eliminate sulfate ions. Then, the dual adsorbent-immobilized sodium silicate was air dried in an oven at 333 K and powdered using a mortar and pestle [47].

2.10. Batch experiments with synthetic dye wastewater using various immobilized dual adsorbents

The required amount of different compositions of various immobilized dual adsorbents was added to the CR dye solution of concentration 300 mg L⁻¹. The dye solutions were stirred at 180 rpm for a required contact time at 303 K. The effluent samples were collected and analyzed for dye concentration in aqueous solution. The suitable matrix for the immobilization of dual adsorbent was selected based on maximum percentage adsorption and mechanical stability. The percentage adsorption in dye solution and effectiveness factor [19,32] were determined using Eqs. (11) and (12), respectively.

$$\% \text{ CR dye adsorption} = \frac{(C_o - C_t) \times 100}{C_o} \quad (11)$$

$$\text{Effectiveness factor} = \frac{\% \text{ adsorption of CR dye by immobilized dual adsorbent}}{\% \text{ adsorption of CR dye by free dual adsorbent}} \quad (12)$$

2.11. Column experiments with synthetic dye wastewater using immobilized DB-WB dual adsorbent

A known amount of suitable immobilized dual adsorbent (immobilized dead biomass-wheat bran) was packed in the column to obtain a bed height of 2 cm. An aqueous CR dye solution of 10 mg L⁻¹ concentration at pH 6 was pumped at a flow rate of 1 mL min⁻¹ using a peristaltic pump [41]. The column study with immobilized dual adsorbent was performed by following the same procedure as given in section 2.6.

2.12. Reusability of free and immobilized dual adsorbents for CR dye adsorption in column studies

After the saturation of the surface of the dual adsorbent, the adsorbate was desorbed from the free and immobilized dual adsorbents by adding the desorbing agent, methanol [52]. The desorption experiments were conducted separately twice using fresh solvent in an Erlenmeyer flask.

After desorption, the free and immobilized dual adsorbents were collected by centrifugation, washed with distilled water, and left to dry at 333 K for 10 h [32]. The regenerated free and immobilized dual adsorbents were reused separately for three runs in column experiments. The percentage adsorption of each regenerated dual adsorbent was tested and compared to the first use. The column experimental procedure was the same as mentioned before in section 2.6.

2.13. Physico-chemical analysis of textile industrial dye effluent

The industrial CR dye effluent was collected from Bright Traders, Erode District, Tamilnadu State, India. The physicochemical characteristics are presented for the month of March 2017. The physicochemical parameters such as pH, turbidity, total suspended solids (TSS), total dissolved solids (TDS), biological oxygen demand (BOD), chemical oxygen demand (COD), total alkalinity, total hardness, electrical conductivity, dissolved oxygen concentration (DO), sulfates, chlorides, sulfides, nitrates, phosphates, calcium, iron, oil and grease were analyzed according to standard operating procedures suitable for wastewater samples [53,54,55,56]. The methodology of this study is presented in Table 1.

3. Results and discussion

3.1. Analysis of column experiments with synthetic dye wastewater using free DB-WB dual adsorbent

Adsorption of CR dye is represented as BTC (i.e., C_t/C_o vs. t). The results show that adsorption of dye onto the dual adsorbent was rapid due to the binding capacity of the pores. Initially the effluent was almost free of solute. As the dye solution continued to flow, the uptake became less effective due to gradual saturation of the binding sites. The effluent concentration started to rise until the bed was exhausted. The shape of the BTC followed a sigmoidal trend [33].

3.1.1. Effect of bed height

The effect of bed height on the CR dye adsorption was analyzed by varying the bed height from 2 to 4 cm. To produce different bed heights of 2, 3 and 4 cm, various amounts of dual adsorbent, that is, 2.97, 4.45 and 5.94 g, were added to the column. The inlet adsorbate concentration (10 mg L⁻¹) and flow rate (1 mL min⁻¹) were fixed. The t_B and t_E increased with increasing bed height (t_B and t_E are correlated with bed height) as shown in Fig. 2. An increase in bed height results in a longer distance for the mass transfer zone to reach the exit and therefore an increase in the t_B [57]. The results of adsorption at various bed heights which are described here are presented in Table 2. The percentage adsorption of CR increased from 78.69% to 84.7% with an increase in bed height from 2 to 4 cm. CR dye has sufficient contact time with the dual adsorbent, which in turn resulted in better adsorption. Therefore, the higher bed depth resulted in a decrease in the adsorbate concentration in the effluent because an increase in the surface area of the dual adsorbent provided more active sites

Table 1
Methodology to analyze the textile industrial effluent using standard operating procedures [53,54,55,56]

Sl. No	Physico-chemical parameters	Method/Instrument
1	pH	Digital pH meter, Systronics
2	Turbidity, NTU	Nephelometric turbidimeter, Systronics
3	Total suspended solids, mg L ⁻¹	Gravimetric method, oven drying at 378 K
4	Total dissolved solids, mg L ⁻¹	Gravimetric method, oven drying at 378 K
5	Biological oxygen demand, mg L ⁻¹	Incubating the sample at 303 K for 5 days followed by titration
6	Chemical oxygen demand, mg L ⁻¹	Closed reflux method
7	Total alkalinity, mg L ⁻¹	Acid-base titration
8	Total hardness, mg L ⁻¹	Complexometric titration
9	Electrical conductivity, mS cm ⁻¹	Conductivity meter, Digisun
10	Dissolved oxygen concentration, mg L ⁻¹	Dissolved oxygen meter, Systronics
11	Sulphates, mg L ⁻¹	Titrimetric method
12	Chlorides, mg L ⁻¹	Argentometric titration
13	Sulphides, mg L ⁻¹	Iodometric method
14	Nitrates, mg L ⁻¹	UV/visible spectrophotometer, Shimadzu
15	Phosphates, mg L ⁻¹	UV/visible spectrophotometer, Shimadzu
16	Calcium, mg L ⁻¹	Complexometric titration
17	Iron, mg L ⁻¹	UV/visible spectrophotometer, Shimadzu
18	Oil and grease, mg L ⁻¹	Partition-gravimetric method

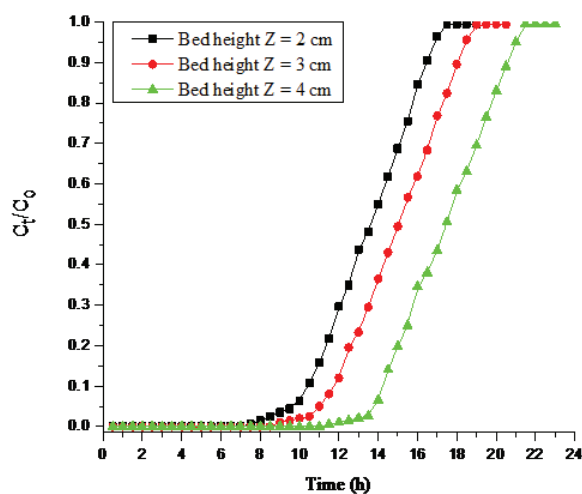


Fig. 2. BTCs for CR dye adsorption onto dual adsorbent at various bed heights. (Inlet adsorbate concentration: 10 mg L⁻¹; initial pH: 6; flow rate: 1 mL min⁻¹; temperature: 303 K).

available for adsorption that resulted in a broadened mass transfer zone [40,58].

3.1.2. Effect of flow rate

The effect of flow rate on the CR dye adsorption was analyzed by varying the flow rate from 1 to 5 mL min⁻¹. The inlet adsorbate concentration (10 mg L⁻¹) and bed height (2 cm) were kept constant. The results of adsorption at various flow rates which are explained here are shown in Table 2. It shows that the adsorption of dye

was dependent mainly on the flow rate. From Fig. 3, both the t_B and t_E decreased with increasing flow rate. The percentage adsorption of CR decreased from 78.69% to 61.40% with an increase in flow rate from 1 to 5 mL min⁻¹, possibly due to insufficient contact time for the adsorbate molecules with the dual adsorbent inside the column and diffusional limitation of the solute into the pores of the dual adsorbent. The BTCs became steeper as the flow rate is increased, and the equilibrium dye uptake (q_e) in the column was lower. A similar observation has been reported elsewhere [40].

3.1.3. Effect of the inlet adsorbate concentration

The effect of the inlet adsorbate concentration on the CR dye adsorption was studied by varying the feed concentration from 10 to 50 mg L⁻¹. The bed height (2 cm) and flow rate (1 mL min⁻¹) were kept constant. Fig. 4 illustrates that the t_B and t_E decreased with increasing inlet CR dye concentration. The column experimental data obtained at various inlet adsorbate concentrations are given in Table 2. The equilibrium dye uptake (q_e) in the column and dye removal percentage increased with increasing feed concentration. The amount of CR adsorbed in the column increased from 8.145 to 16.95 mg and the percentage adsorption increased from 78.69% to 81.45% with an increase in the inlet adsorbate concentration from 10 to 50 mg L⁻¹. Also, the steep BTC was obtained at high inlet adsorbate concentration. The increase in feed concentration leads to an increase in the concentration gradient between the adsorbate in solution and in the adsorbent. Due to the high concentration gradient, a better amount of dye uptake in the column was obtained [31,33]. The above result demonstrated that the change in concentration gradient affected the CR dye loading rate and t_B . The

Table 2
Effect of bed height, flow rate and influent adsorbate concentration on CR dye adsorption

Z (cm)	Q (mL min ⁻¹)	C _o (mg L ⁻¹)	t _b (h)	t _E (h)	m _{ad} (mg)	m _{total} (mg)	V _{eff} (L)	q _e (mg g ⁻¹)	% dye removal
2	1	10	7.25	17.25	8.14	10.35	1.03	2.74	78.69
3	1	10	8.50	19.00	13.89	17.12	1.14	3.12	81.13
4	1	10	11.00	21.50	20.93	24.71	1.29	3.52	84.70
2	1	10	7.25	17.25	8.14	10.35	1.03	2.74	78.69
2	3	10	4.50	14.50	6.58	9.49	2.61	2.21	69.33
2	5	10	2.50	11.00	5.33	8.68	3.30	1.79	61.40
2	1	10	7.25	17.25	8.14	10.35	1.03	2.74	78.69
2	1	20	4.00	13.00	11.51	14.32	0.78	3.88	80.34
2	1	50	2.00	7.00	16.95	20.81	0.42	5.71	81.45

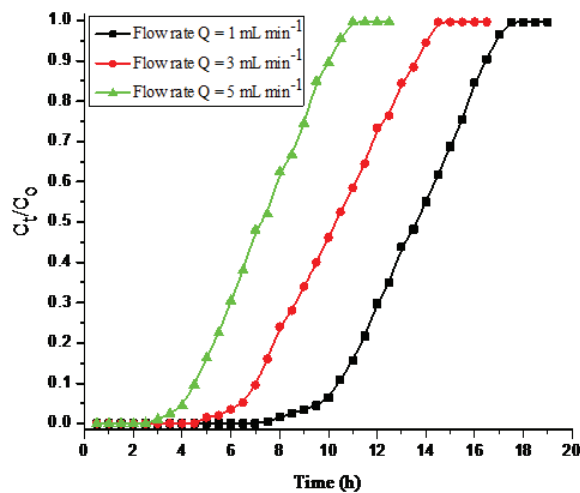


Fig. 3. BTCs for CR adsorption onto dual adsorbent at various flow rates. (Inlet adsorbate concentration: 10 mg L⁻¹; initial pH: 6; bed height: 2 cm; temperature: 303 K).

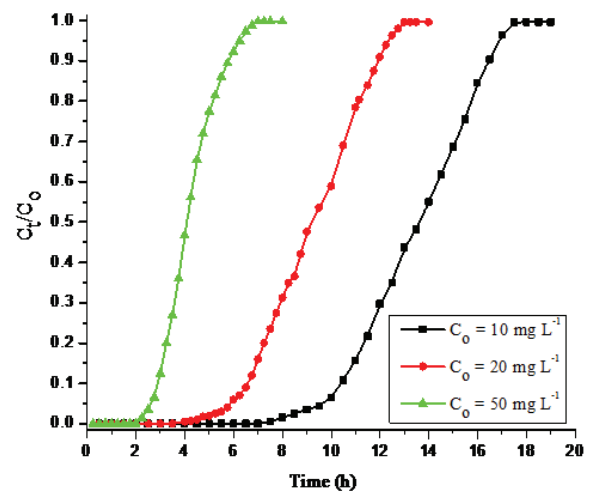


Fig. 4. BTCs for CR adsorption onto dual adsorbent at various influent adsorbate concentrations. (Initial pH: 6; bed height: 2 cm; flow rate: 1 mL min⁻¹; temperature: 303 K).

increase in the mass of dye adsorbed in the column can be described by more binding sites being occupied as the inlet adsorbate concentration increased [59,60].

3.2. Evaluation and estimation of BTCs with kinetic constants in various models

3.2.1. Adams-Bohart model

The Adams-Bohart model equation was applied to the column experimental data for the analysis of BTC. The characteristic parameters (model constants) are reported in Table 3. The values of K_{AB} and N_o were influenced by bed heights, flow rates and inlet adsorbate concentrations. The kinetic constant K_{AB} increased with increasing flow rate, showing that the overall rate of the dye adsorption process is governed by external mass transfer [33]. The maximum saturation concentration N_o increased with increasing adsorbate concentration and bed height. The predicted and experimental BTCs with respect to various bed heights, flow rates and adsorbate concentrations are

Table 3

Adams-Bohart model parameters under various operating conditions for CR dye adsorption

Z (cm)	Q (mL min ⁻¹)	C _o (mg L ⁻¹)	K _{AB} (L mg ⁻¹ min ⁻¹)	N _o (mg L ⁻¹)	R ²
2	1	10	7.93 × 10 ⁻⁴	1390.67	0.836
3	1	10	7.67 × 10 ⁻⁴	2118.39	0.864
4	1	10	6.45 × 10 ⁻⁴	3083.67	0.913
2	3	10	8.12 × 10 ⁻⁴	1246.54	0.903
2	5	10	8.36 × 10 ⁻⁴	1098.32	0.897
2	1	20	4.54 × 10 ⁻⁴	1987.46	0.922
2	1	50	2.32 × 10 ⁻⁴	2578.67	0.864

shown in Figs. 5–7. Large differences were found between the predicted and experimental BTCs. The linear regression coefficient, R², values were in the range between 0.836–0.922, suggesting that this model was not fitting the data points very well.

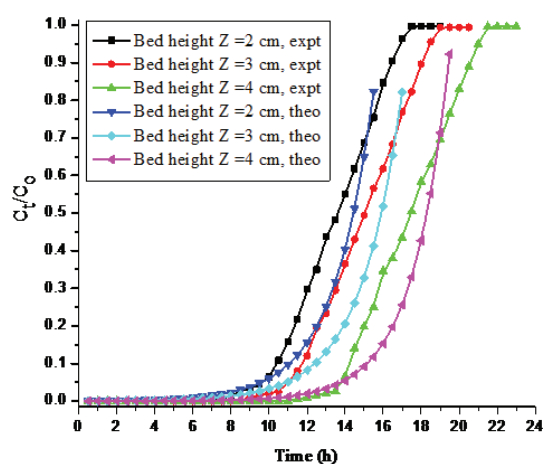


Fig. 5. BTCs for real-time versus the simulated Adams-Bohart model at various bed heights. (Inlet adsorbate concentration: 10 mg L^{-1} ; initial pH: 6; flowrate: 1 mL min^{-1} ; temperature: 303 K).

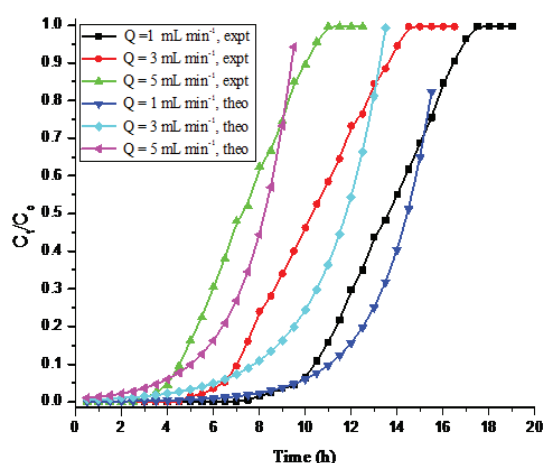


Fig. 6. BTCs for real-time versus the simulated Adams-Bohart model at various flowrates. (Inlet adsorbate concentration: 10 mg L^{-1} ; initial pH: 6; bed height: 2 cm ; temperature: 303 K).

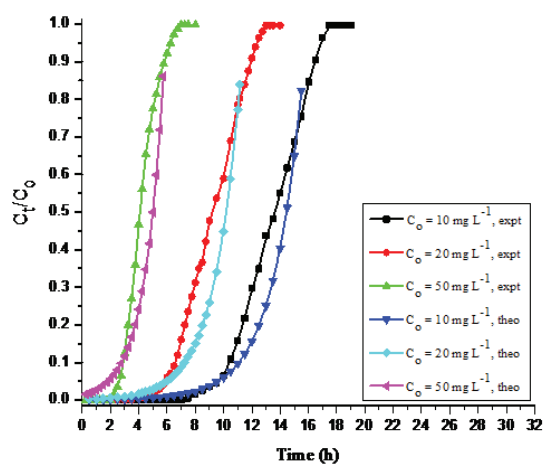


Fig. 7. BTCs for real-time versus the simulated Adams-Bohart model at various adsorbate concentrations. (Initial pH: 6; bed height: 2 cm ; flowrate: 1 mL min^{-1} ; temperature: 303 K).

3.2.2. Bed depth service time (BDST) model

The BDST model equation was applied to the experimental data for the description of BTC. The model constants were evaluated and are reported in Table 4, showing that the value of K increased with increasing flow rate. The rate constant K characterizes the rate of solute transfer from a liquid to a solid phase. This model ignores the pore and external film diffusion resistance so that the solute is loaded onto the dual adsorbent [40]. The value of N_0 increased with increasing adsorbate concentration and bed height. The predicted and experimental BTCs with respect to various bed heights, flow rates and adsorbate concentrations are shown in Figs. 8–10. There was a small deviation between experimental and predicted BTCs. Also, the R^2 values were in the range between 0.954–0.988, indicating that this model was not completely fitting the column experimental data.

3.2.3. Thomas model

The column experimental data were fitted to the Thomas model equation to evaluate the kinetic constants, and their values are reported in Table 5. This model is one of the most general and widely used theoretical methods

Table 4
Bed depth service time model parameters at various operating conditions for CR dye adsorption

Z (cm)	Q (mL min^{-1})	C_0 (mg L^{-1})	K ($\text{L mg}^{-1} \text{min}^{-1}$)	N_0 (mg L^{-1})	R^2
2	1	10	1.45×10^{-3}	1149.17	0.954
3	1	10	1.38×10^{-3}	1353.92	0.977
4	1	10	1.29×10^{-3}	1564.26	0.976
2	3	10	1.53×10^{-3}	936.48	0.966
2	5	10	1.72×10^{-3}	624.72	0.969
2	1	20	8.16×10^{-4}	1575.03	0.985
2	1	50	5.90×10^{-4}	1852.44	0.988

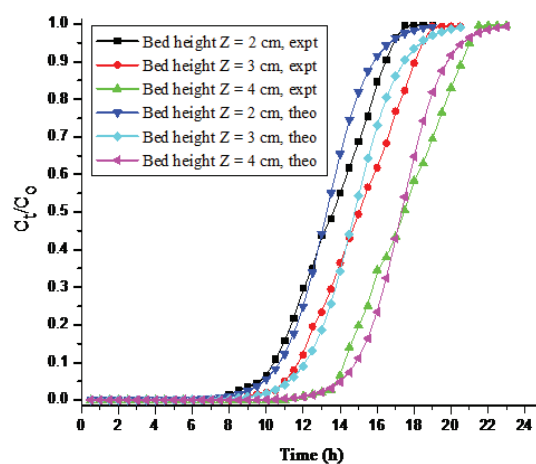


Fig. 8. BTCs for real-time versus the simulated BDST model at various bed heights. (Inlet adsorbate concentration: 10 mg L^{-1} ; initial pH: 6; flowrate: 1 mL min^{-1} ; temperature: 303 K).

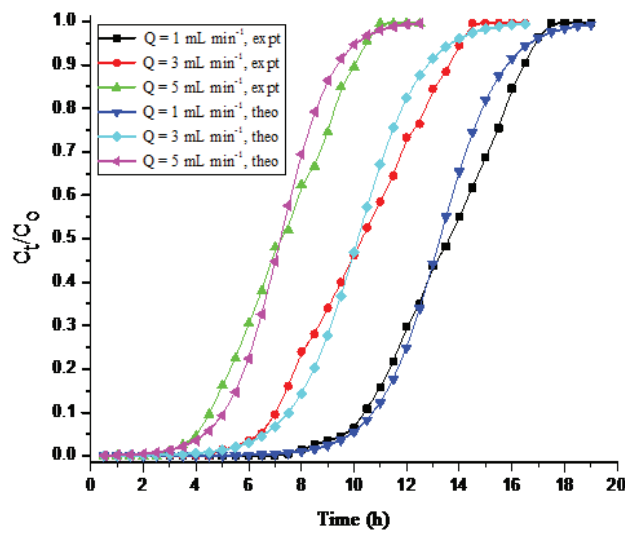


Fig. 9. BTCs for real-time versus the simulated BDST model at various flow rates. (Inlet adsorbate concentration: 10 mg L⁻¹; initial pH: 6; bed height: 2 cm; temperature: 303 K).

to describe the column performance [33]. From Table 5, as the inlet adsorbate concentration increased, the values of K_{Th} decreased and the values of q_{oTh} increased. The same trend was observed as the bed height was increased. The maximum uptake of CR in the solid phase (q_{oTh}) decreased and the values of K_{Th} increased with increasing flow rate, indicating that the overall system kinetics was controlled by external film diffusion [33]. The predicted and experimental BTCs with respect to various bed heights, flow rates and adsorbate concentrations are shown in Figs. 11–13. BTCs predicted from this model are in good agreement with the experimental data. Also, the calculated values of q_{oTh} were close to the experimental values of q_{oTh} under different operating conditions. The regression coefficient, R^2 , ranging from 0.967 to 0.999 indicates that this model is valid for CR adsorption. This model assumes that the external and pore diffusions are not the rate-controlling step, Langmuir kinetics of adsorption are valid, and no axial dispersion is derived with the adsorption. However, adsorption is usually not limited by chemical reaction kinetics but is often controlled by interphase mass transfer, and the effect of axial dispersion may be important at lower flow rates [33].

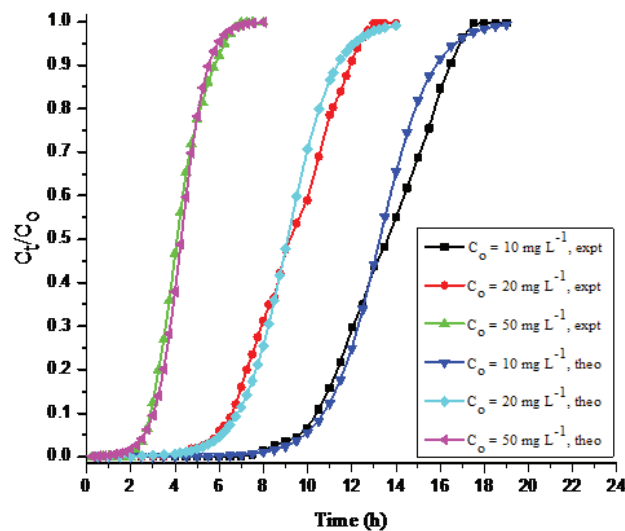


Fig. 10. BTCs for real-time versus the simulated BDST model at various adsorbate concentrations. (Initial pH: 6; bed height: 2 cm; flow rate: 1 mL min⁻¹; temperature: 303 K).

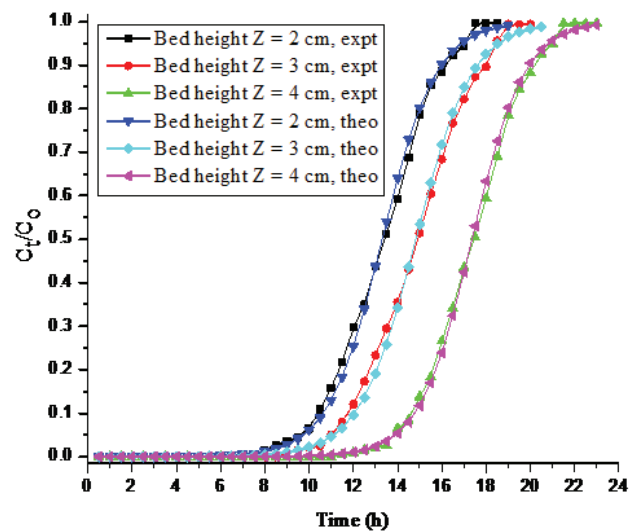


Fig. 11. BTCs for real-time versus the simulated Thomas model at various bed heights. (Inlet adsorbate concentration: 10 mg L⁻¹; initial pH: 6; flow rate: 1 mL min⁻¹; temperature: 303 K).

Table 5
Thomas model parameters at various operating conditions for CR dye adsorption

Z (cm)	Q (mL min ⁻¹)	C ₀ (mg L ⁻¹)	K _{Th} (L mg ⁻¹ min ⁻¹)	q _{oTh, expt} (mg g ⁻¹)	q _{oTh, calc} (mg g ⁻¹)	R ²
2	1	10	1.38 × 10 ⁻³	2.69	2.84	0.985
3	1	10	1.16 × 10 ⁻³	2.98	3.14	0.989
4	1	10	8.70 × 10 ⁻⁴	3.51	3.69	0.976
2	3	10	4.30 × 10 ⁻³	2.27	2.63	0.967
2	5	10	8.71 × 10 ⁻³	1.75	1.82	0.969
2	1	20	8.92 × 10 ⁻⁴	3.68	3.92	0.984
2	1	50	5.80 × 10 ⁻⁴	4.32	4.48	0.999

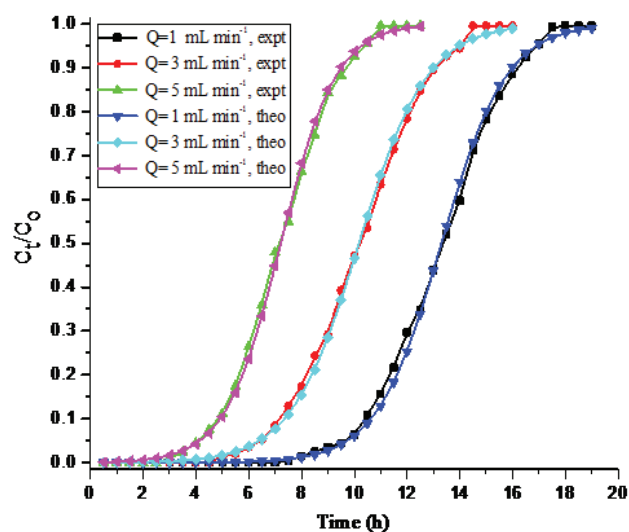


Fig. 12. BTCs for real-time versus the simulated Thomas model at various flow rates. (Inlet adsorbate concentration: 10 mg L⁻¹; initial pH: 6; bed height: 2 cm; temperature: 303 K).

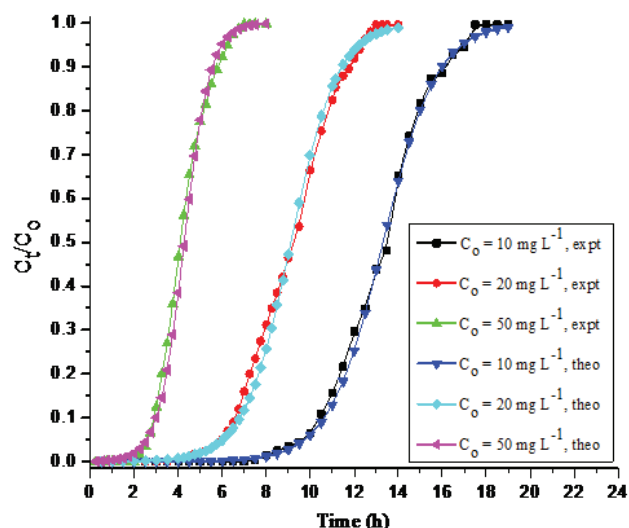


Fig. 13. BTCs for real-time versus the simulated Thomas model at various adsorbate concentrations. (Initial pH: 6; bed height: 2 cm; flow rate: 1 mL min⁻¹; temperature: 303 K).

3.2.4. Yoon-Nelson model

The Yoon-Nelson model equation was applied to analyze the breakthrough behavior of CR onto the dual adsorbent. The model constants were evaluated under various operating conditions, and the values are reported in Table 6. Table 6 shows that the value of k_{YN} increased and τ decreased with increasing flow rate and adsorbate concentration. The opposite trend was observed as the bed height was increased. The predicted and experimental BTCs at various bed heights, flow rates and adsorbate concentrations are shown in Figs. 14–16. The predicted BTCs and calculated bed capacity (q_{oYN}) were close to experimental values. This is proven by the high values of the regression coefficient, R^2 , ranging from 0.969 to 0.999, which suggests that this model is valid for CR adsorption. The values of τ from the calculation were like the experimental values under different operating conditions. In general, the Yoon-Nelson model is capable of modeling symmetric BTCs and neglects the effect of axial dispersion [33].

From the above experimental results and regression co-efficients, R^2 , the Thomas and Yoon-Nelson model were demonstrated to provide a good correlation of the effects of bed height, flow rate and inlet adsorbate concentration.

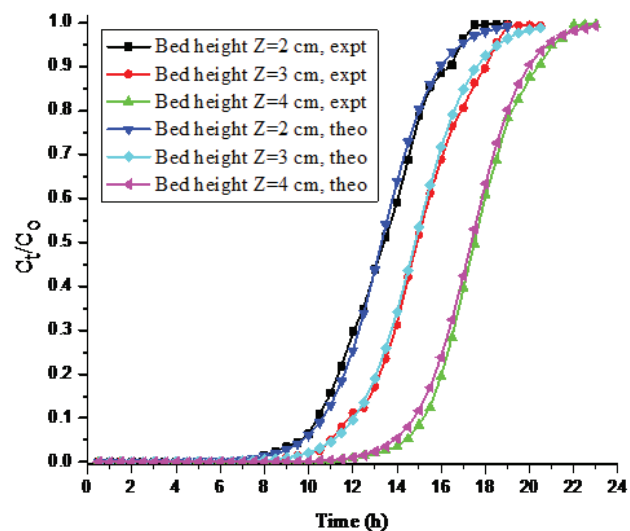


Fig. 14. BTCs for real-time versus the simulated Yoon-Nelson model at various bed heights. (Inlet adsorbate concentration: 10 mg L⁻¹; initial pH: 6; flow rate: 1 mL min⁻¹; temperature: 303 K).

Table 6
Yoon–Nelson model parameters at various operating conditions for CR dye adsorption

Z (cm)	Q (mL min ⁻¹)	C _o (mg L ⁻¹)	K _{YN} (min ⁻¹)	q _{oYN^{expt}} (mg g ⁻¹)	q _{oYN,calc} (mg g ⁻¹)	τ _{expt} (min)	τ _{calc} (min)	R ²
2	1	10	0.0138	2.688	2.734	798.37	811.99	0.987
3	1	10	0.0097	2.942	2.963	1310.66	1320.01	0.989
4	1	10	0.0083	3.258	3.422	1965.28	2032.66	0.986
2	3	10	0.0352	1.956	2.134	193.64	211.27	0.974
2	5	10	0.0647	1.463	1.654	86.90	98.06	0.969
2	1	20	0.0163	3.574	3.628	530.74	548.76	0.995
2	1	50	0.0274	4.926	5.012	292.60	297.71	0.999

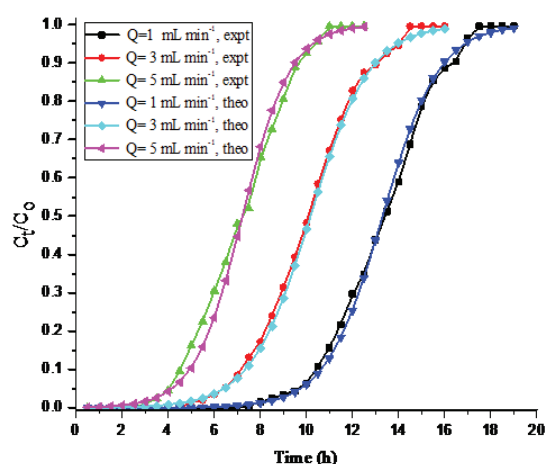


Fig. 15. BTCs for real-time versus the simulated Yoon-Nelson model at various flow rates. (Inlet adsorbate concentration: 10 mg L⁻¹; initial pH: 6; bed height: 2 cm; temperature: 303 K).

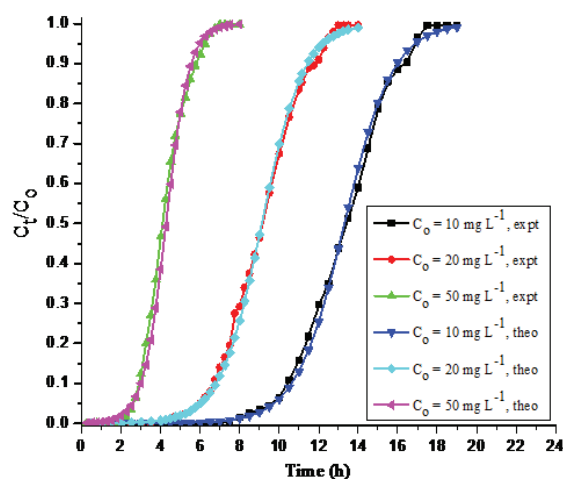


Fig. 16. BTCs for real-time versus the simulated Yoon-Nelson model at various adsorbate concentrations. (Initial pH: 6; bed height: 2 cm; flowrate: 1 mL min⁻¹; temperature: 303 K).

3.3 Evaluation of a suitable matrix for immobilization of the DB-WB dual adsorbent

To optimize dual adsorbent loading in each polymeric matrix, immobilized adsorbents were prepared with varying compositions of dual adsorbent in each matrix. The results of adsorption experiments obtained by using different immobilized matrices with varying dual adsorbent loading are reported in Table 7. For all matrices compared, an increase in dual adsorbent loading yields better adsorption. However, loading above an optimal limit decreases the percentage dye adsorption, which may be attributed to the difference in porosity of the beads (beads/gel may be less porous) when a higher quantity of dual adsorbent was loaded. As the dual adsorbent dose was increased in various matrices, the loading may affect the free transport of dye anions to the interior binding sites through the formation of a physical boundary layer. This phenomenon may be explained by the agglomeration of dual adsorbent particles in various polymeric matrices [32], or may also be due to the screening effect of the denser dual adsorbent at the outer layer of the immobilized matrix [61]. The optimum dual adsorbent loading was found to be 4% (w/v) for calcium alginate, 5% (w/v) for polyvinyl alcohol, 8% (w/v) for polysulfone and 2.5% (w/v) for sodium silicate. The CR dye adsorption efficiencies on various immobilized dual adsorbents were compared with the adsorption efficiencies on the free dual adsorbent. The effectiveness factor was determined to be on the order of free dual adsorbent (1) > sodium silicate (0.857) > calcium alginate (0.835) > polysulfone (0.816) > polyvinyl alcohol (0.794) with an initial adsorbate concentration of 100 mg L⁻¹. The various immobilized dual adsorbent matrices (except sodium silicate gel) were adhering together to form clumps during both adsorption and desorption cycles in aqueous media [32]. This property is encountered with the effective water flow when packed in column reactors. Among the various immobilized polymeric matrices, sodium silicate was chosen as the superior matrix. The sodium silicate matrix was found to exhibit better results (84.72% CR dye adsorption) and the lowest cost of the polymeric

Table 7
Effect of dual adsorbent composition in various polymeric matrices for CR dye adsorption

Dual adsorbent loading % (w/v)	% adsorption of CR dye in various immobilized polymeric matrices			
	Calcium alginate	Polyvinyl alcohol	Polysulfone	Sodium silicate
1	72.48	60.36	70.64	77.99
1.5	74.26	65.30	71.97	80.92
2	75.69	69.65	74.10	83.60
2.5	77.54	72.94	75.26	84.72
3	80.26	74.68	76.39	82.89
4	82.58	76.34	77.63	78.55
5	81.15	78.52	78.24	73.12
6	79.34	77.16	79.46	69.63
8	76.28	73.38	80.67	62.37
9	73.35	69.08	78.12	58.15
10	71.14	63.44	77.56	54.29

(Initial adsorbate concentration: 300 mg L⁻¹; volume of dye solution: 100 mL; pH: 6; immobilized dual adsorbent dosage: 0.5 g; agitation speed: 180 rpm; temperature: 303 K; contact time: 24 h).

materials. Therefore, further column experiments were conducted using the optimized value of dual adsorbent loading in the sodium silicate matrix.

3.4. Reusability of free and immobilized dual adsorbents for CR dye adsorption in column studies

Studies pertaining to CR dye adsorption were carried out in three runs with free and immobilized dual adsorbent separately. The column experimental results are reported in Table 8. The t_b and t_E decreased significantly after the first run, showing that the treated effluent volume and percentage adsorption of the regenerated dual adsorbent decreased during the second and third runs compared to the first due to insufficient desorption of the bound dye anions from the dual adsorbent surface (the dual adsorbent active site are almost blocked with CR dye molecules) and lack of binding sites on the solid adsorbent. The percentage adsorption and equilibrium dye uptake using immobilized dual adsorbent in all three runs were lower than when free dual adsorbent was used, possibly because of the formation of a physical boundary layer around the immobilized matrix. The matrix thereby impedes the accessibility of dye anions to the binding sites of the dual adsorbent [32,50]. The percentages of

dye adsorption were 57.75% and 41.70%; equilibrium dye uptakes were 0.696 mg g^{-1} and 0.35 mg g^{-1} in the third run of operation with free and immobilized dual adsorbent, respectively. The constants found from all of the various modeling equations are reported in Tables 9 and 10. Tables 9 and 10 show that the values of constants from all of the various model equations decreased with increasing number of runs. A similar observation has been reported elsewhere [42,62,63]. Considering the regression coefficient, R^2 , values, the Thomas and Yoon-Nelson models fitted well with the column experimental data. The BTCs for adsorption of CR onto free and immobilized dual adsorbents in various runs are shown in Figs. 17–18.

3.5. Physico-chemical analysis of textile industrial CR dye effluent in batch studies

The physicochemical parameters of the real and treated textile industrial effluent have been analyzed, and the batch experimental results were compared with the Central Pollution Control Board (CPCB) standard limits. All of the data were recorded twice, and the average values are reported in Table 11. The characteristics of the raw effluent were higher than the standard prescribed by the CPCB.

Table 8

Column experimental parameters obtained at various runs for the adsorption of CR dye onto free and immobilized dual adsorbents

Runs	Free dual adsorbent										Immobilized dual adsorbent								
	Z (cm)	W (g)	t_b (h)	t_E (h)	m_{ad} (mg)	m_{total} (mg)	V_{eff} (L)	q_e (mg g^{-1})	% adsorption	Z (cm)	W (g)	t_b (h)	t_E (h)	m_{ad} (mg)	m_{total} (mg)	V_{eff} (L)	q_e (mg g^{-1})	% adsorption	
1	2	2.97	7.25	17.25	8.145	10.35	1.035	2.74	78.69	2	2.69	5.00	12	4.628	7.20	0.720	1.72	64.27	
2	1.8	2.68	4.50	11.75	4.680	7.05	0.705	1.75	66.38	1.75	2.35	2.50	8.50	2.837	5.10	0.510	1.21	55.63	
3	1.67	2.485	2.00	5.00	1.732	3.00	0.300	0.696	57.75	1.59	2.14	1	2.75	0.688	1.65	0.165	0.35	41.70	

Table 9

Column characteristic parameters obtained at various runs for the adsorption of CR onto free dual adsorbent

Runs	Adams-Bohart model			BDST model			Thomas model			Yoon-Nelson model		
	K_{AB} ($\text{L mg}^{-1}\text{min}^{-1}$)	N_o (mg L^{-1})	R^2	K ($\text{L mg}^{-1}\text{min}^{-1}$)	N_o (mg L^{-1})	R^2	K_{TH} ($\text{mL mg}^{-1}\text{min}^{-1}$)	q_{oTH} (mg g^{-1})	R^2	K_{YN} (min^{-1})	τ (min)	R^2
1	7.93×10^{-4}	1390.6	0.856	1.452×10^{-3}	1149.17	0.954	1.38	2.69	0.985	0.0142	798.4	0.987
2	5.24×10^{-4}	1025.0	0.884	1.064×10^{-3}	807.28	0.962	0.74	1.88	0.994	0.0082	505.4	0.996
3	2.06×10^{-4}	584.25	0.872	0.738×10^{-3}	436.92	0.967	0.45	0.75	0.997	0.0056	188.1	0.998

Table 10

Column characteristic parameters obtained at various runs for the adsorption of CR by immobilized dual adsorbent

Runs	Adams-Bohart model			BDST model			Thomas model			Yoon-Nelson model		
	K_{AB} ($\text{L mg}^{-1}\text{min}^{-1}$)	N_o (mg L^{-1})	R^2	K ($\text{L mg}^{-1}\text{min}^{-1}$)	N_o (mg L^{-1})	R^2	K_{TH} ($\text{mL mg}^{-1}\text{min}^{-1}$)	q_{oTH} (mg g^{-1})	R^2	K_{YN} (min^{-1})	τ (min)	R^2
1	7.35×10^{-4}	936.8	0.903	1.96×10^{-3}	720.30	0.964	0.962	1.84	0.976	0.0121	497.2	0.977
2	2.76×10^{-4}	730.4	0.882	1.15×10^{-3}	506.33	0.945	0.533	1.27	0.989	0.0063	245.6	0.989
3	1.18×10^{-4}	287.4	0.798	0.56×10^{-3}	274.71	0.926	0.224	0.56	0.984	0.0037	89.5	0.986

Table 11
Characteristics of real and treated textile industrial CR dye effluent with acceptable limits

Sl. No	Parameters	Real effluent value	Treated effluent value	CPCB standard
1	pH	8.64	8.50	6–9
2	Turbidity, NTU	153	22	10
3	Total suspended solids, mg L ⁻¹	43	18	100
4	Total dissolved solids, mg L ⁻¹	3786	934	2000
5	Biological oxygen demand, mg L ⁻¹	638	52	30
6	Chemical oxygen demand, mg L ⁻¹	1824	246	250
7	Total alkalinity, mg L ⁻¹	420	65	200
8	Total hardness, mg L ⁻¹	764	430	300
9	Electrical conductivity, mS cm ⁻¹	5.28	5.13	2.25
10	Dissolved oxygen concentration, mg L ⁻¹	1.12	1.05	4
11	Sulphates, mg L ⁻¹	560	126	250
12	Chlorides, mg L ⁻¹	1526	214	500
13	Sulphides, mg L ⁻¹	182	90	2
14	Nitrates, mg L ⁻¹	24	2.62	50
15	Phosphates, mg L ⁻¹	4.36	1.25	20
16	Calcium, mg L ⁻¹	120	36	200
17	Iron, mg L ⁻¹	0.12	0.064	3
18	Oil and grease, mg L ⁻¹	11	4.54	10

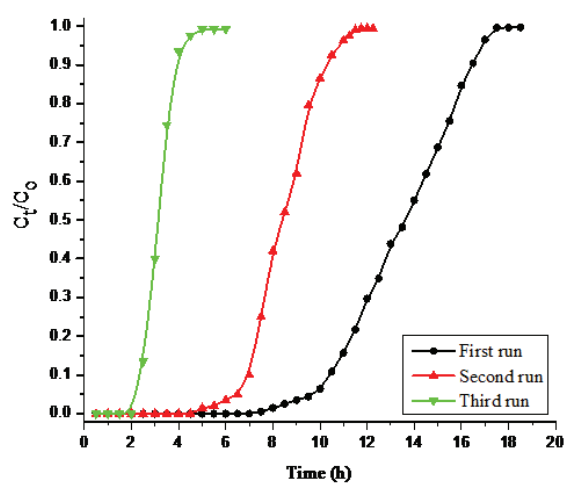


Fig. 17. BTCs for adsorption of CR dye onto free dual adsorbent in various runs. (Inlet adsorbate concentration: 10 mg L⁻¹; initial pH: 6; flow rate: 1 mL min⁻¹; temperature: 303 K).

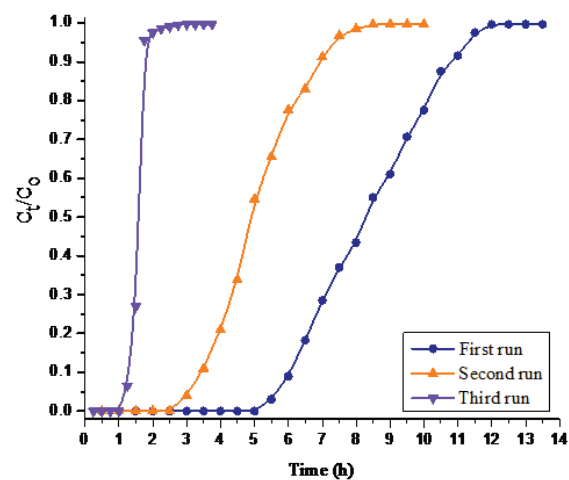


Fig. 18. BTCs for adsorption of CR dye by immobilized dual adsorbent in various runs. (Inlet adsorbate concentration: 10 mg L⁻¹; initial pH: 6; flow rate: 1 mL min⁻¹; temperature: 303 K).

The effluent was highly turbid and colored with average organic and inorganic loading. The pH of the raw industrial dye effluent was 8.64, which indicates that the effluents from dyeing industries under study area are alkaline in nature, indicating that different types of chemicals such as NaOCl, Na₂CO₃, NaHCO₃, NaOH, surfactants and sodium phosphate were used during the processing steps [64]. The value of COD for a given dye effluent was 1824 mg L⁻¹, which is higher than the CPCB standard. The higher value of COD is especially from the dyeing section of the textile processing industry because of the nature of the chemicals employed. The ratio of BOD:COD was also studied, and if the BOD:COD ratio was less than 0.5, the effluent con-

tained a large proportion of non-biodegradable matter [65]. The ratio of the BOD:COD obtained from the result was 0.35, indicating that the effluent contains a large portion of non-biodegradable matter. However, the characteristics of treated industrial dye effluent using dual adsorbent were closer to standard values.

3.6. Analysis of column experiments with textile industrial CR dye effluent using free and immobilized DB-WB dual adsorbents

The column adsorption experiments were conducted separately with industrial dye effluents using free and immobilized dual adsorbents. The inlet adsorbate concen-

Table 12

Column experimental parameters for the adsorption of solute onto free and immobilized dual adsorbents with industrial CR dye effluent

Adsorbent	W (g)	t_b (h)	t_E (h)	m_{ad} (mg)	m_{total} (mg)	V_{eff} (L)	q_e (mg g ⁻¹)	% adsorption
Free dual adsorbent	2.97	0.5	3.25	32.05	39	0.195	10.79	82.18
Immobilized dual adsorbent	2.69	0.25	2.75	22.22	33	0.165	8.26	67.34

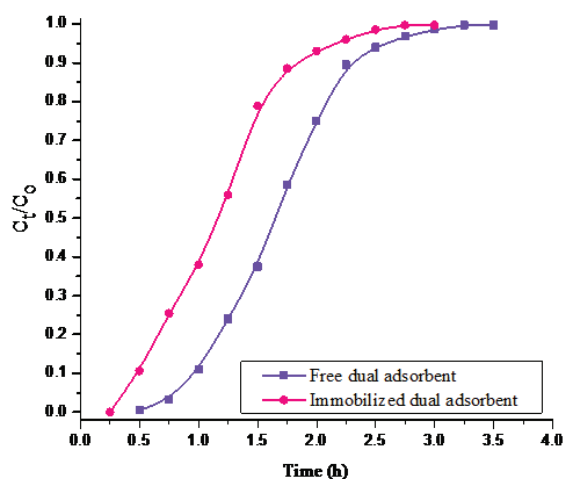


Fig. 19. BTCs for adsorption of solute onto free and immobilized dual adsorbents with textile industrial CR dye effluent. (Bed height: 2 cm; inlet adsorbate concentration: 200 mg L⁻¹; initial pH: 6; flow rate: 1 mL min⁻¹; temperature: 303 K).

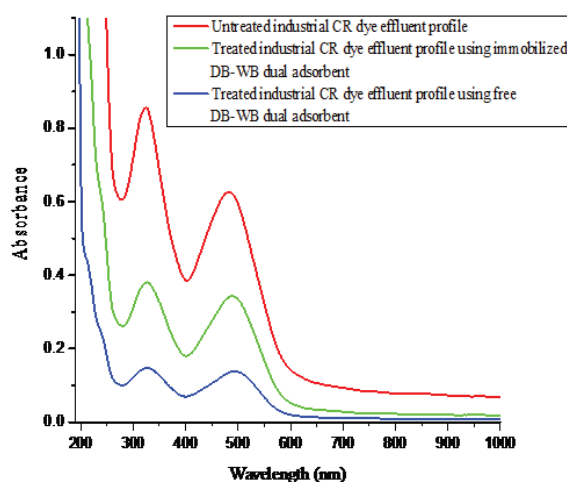


Fig. 20. Industrial CR dye effluent adsorption profile obtained in column studies using free and immobilized DB-WB dual adsorbents with untreated effluent profile. (Bed height: 2 cm; inlet adsorbate concentration: 200 mg L⁻¹; initial pH: 6; flow rate: 1 mL min⁻¹; temperature: 303 K).

tration was measured and it was found to be 200 mg L⁻¹. The bed height (2 cm) and flow rate (1 mL min⁻¹) were kept constant. The column experimental procedure was the same as given before in section 2.6. The column experimental results are reported in Table 12. While using free and immobilized dual adsorbents, the percentage adsorption of the

industrial dye effluent was more than 60%. The percentages of solute adsorption were 82.18% and 67.34%; equilibrium solute uptakes were 10.79 mg g⁻¹ and 8.26 mg g⁻¹ with free and immobilized dual adsorbent, respectively. While using the immobilized dual adsorbent, the breakthrough point time (t_B), bed exhaustion time (t_E), treated effluent volume (V_{eff}), equilibrium dye uptake (q_e), mass of solute adsorbed (m_{ad}) and percentage adsorption were lower than when free dual adsorbent was used. The BTCs for adsorption of solute from industrial dye effluent with free and immobilized dual adsorbents are shown in Fig. 19. The column reached t_B , t_E faster, and a steep BTC observed at high inlet adsorbate concentration was used. The intensity of the peaks of dye effluent was measured before and after adsorption. The intensity of peaks declined considerably after treatment with both the free and immobilized dual adsorbents (Fig. 20).

4. Conclusion

The filamentous dead fungus *Neurospora crassa* along with wheat bran may be used as an effective adsorbent for the removal of CR dye color from an aqueous solution. The percentage adsorption on free dual adsorbent was found to vary with bed height, flow rate and the inlet adsorbate concentration. The higher the bed depth and inlet adsorbate concentration, the higher is the percentage adsorption. The adsorption percentage declined with an increased flow rate. The equilibrium dye uptake is linearly correlated with bed height and the inlet adsorbate concentration. The opposite trend was observed as the flow rate increased. The breakthrough point time and bed exhaustion time increased with an increase in bed height and decreased with an increase in inlet adsorbate concentration and flow rate. The steep breakthrough curve was observed at high inlet adsorbate concentration. By varying the operating characteristics of the fixed-bed column, for example, bed height, flow rate and inlet adsorbate concentration very rapidly, an efficient CR dye uptake was achieved for the system. The various model equations were applied to column experimental data to estimate the breakthrough curves and evaluate the model constants. While considering the regression coefficient, R^2 , and predicted breakthrough curves, it could well be said that Thomas and Yoon-Nelson models were in accordance with the real-time column experimental data. The overall system kinetics were controlled by external film diffusion. The dead fungal biomass-wheat bran dual adsorbent loading (composition) in various polymeric matrices was optimized for immobilization of dual adsorbent. The suitable polymeric matrix for immobilization of dual adsorbent was identified. Desorption studies were conducted using the desorbing agent methanol to explore the possi-

bility of recovering free and immobilized dual adsorbents. Reusability studies of free and immobilized dual adsorbents for CR dye re-adsorption were carried out in column studies in three separate runs. Decreases in the percentage adsorption and equilibrium dye uptake were observed with increases in the number of runs. The adsorption of solute from textile industrial CR dye effluent was carried out in column studies separately using free and immobilized dual adsorbents. While using the immobilized dual adsorbent, the equilibrium dye uptake and percentage adsorption were lower than when free dual adsorbent was used. The experimental results showed that the prepared material was a useful dual adsorbent for effective adsorption of anionic dyes from industrial effluents.

Symbols and abbreviations

BDST	—	Bed depth service time (sec)
BOD	—	Biological oxygen demand (kg m^{-3})
BP	—	Breakthrough point
BTC	—	Breakthrough curve
CCD	—	Central composite design
COD	—	Chemical oxygen demand (kg m^{-3})
CPCB	—	Central Pollution Control Board
CR	—	Congo red dye
C_o	—	Inlet (feed) dye concentration (kg m^{-3})
C_t	—	Effluent dye concentration (kg m^{-3})
DB-WB	—	Dead biomass-wheat bran dual adsorbent
DO	—	Dissolved oxygen concentration (kg m^{-3})
K	—	Kinetic constant in the BDST model ($\text{m}^3 \text{kg}^{-1} \text{s}^{-1}$)
K_{AB}	—	Kinetic constant in the Adams-Bohart model ($\text{m}^3 \text{kg}^{-1} \text{s}^{-1}$)
K_{Th}	—	Kinetic constant in the Thomas model ($\text{m}^3 \text{kg}^{-1} \text{s}^{-1}$)
k_{YN}	—	Kinetic constant in the Yoon-Nelson model (s^{-1})
m_{ad}	—	Total adsorbed quantity of dye in the column (kg)
m_{total}	—	Total amount of dye fed to the column (kg)
NTU	—	Nephelometric turbidity unit
N_o	—	Maximum saturation concentration (kg m^{-3})
Q	—	Volumetric flow rate ($\text{m}^3 \text{sec}^{-1}$)
q_e	—	Mass of solute adsorbed per kg of dual adsorbent in the column (kg kg^{-1})
q_{oTh}	—	Adsorption capacity of the column in Thomas model (kg kg^{-1})
q_{oYN}	—	Adsorption capacity of the column in Yoon-Nelson model (kg kg^{-1})
R^2	—	Linear regression correlation coefficient
T	—	Temperature (K)
TDS	—	Total dissolved solids (kg m^{-3})
TSS	—	Total suspended solids (kg m^{-3})
t_B	—	Breakthrough point time (s)
t_{total}	—	Total flow time (s)
t_E	—	Bed exhaustion time (s)
U_o	—	Superficial velocity (m s^{-1})
V	—	Volume of CR dye solution (m^3)
V_{eff}	—	Effluent volume (m^3)
W	—	Mass of dry dual adsorbent (kg)
Z	—	Bed height (m)

Greek letters

τ	—	Time required for 50% adsorbate breakthrough (s)
--------	---	--

References

- [1] W. Zhang, H. Yan, H. Li, Z. Jiang, L. Dong, X. Kan, H. Yang, A. Li, R. Cheng, Removal of dyes from aqueous solutions by straw based adsorbents: Batch and column studies, *Chem. Eng. J.*, 168 (2011) 1120–1127.
- [2] R. Malarvizhi, N. Sulochana, Sorption isotherm and kinetic studies of methylene blue uptake onto activated carbon prepared from wood apple shell, *J. Environ. Prot. Sci.*, 2 (2008) 40–46.
- [3] V.S. Munagapati, D.S. Kim, Equilibrium isotherms, kinetics, and thermodynamics studies for congo red adsorption using calcium alginate beads impregnated with nano-goethite, *Ecotoxicol. Environ. Saf.*, 141 (2017) 226–234.
- [4] R. Ahmad, R. Kumar, Adsorptive removal of congo red dye from aqueous solution using bael shell carbon, *Appl. Surf. Sci.*, 257 (2010) 1628–1633.
- [5] A.R. Cestari, E.F.S. Vieira, G.S. Vieira, L.E. Almeida, Aggregation and adsorption of reactive dyes in the presence of an anionic surfactant on mesoporous aminopropyl silica, *J. Colloid Interface Sci.*, 309 (2007) 402–411.
- [6] D. Pathania, A. Sharma, Z.M. Siddiqi, Removal of congo red dye from aqueous system using *Phoenix dactylifera* seeds, *J. Mol. Liq.*, 219 (2016) 359–367.
- [7] S.R. Couto, Dye removal by immobilized fungi, *Biotechnol. Adv.*, 27 (2009) 227–235.
- [8] C. Srilakshmi, R. Saraf, Ag-doped hydroxyapatite as efficient adsorbent for removal of congo red dye from aqueous solutions: synthesis, kinetic and equilibrium adsorption isotherm analysis, *Microporous Mesoporous Mater.*, 219 (2016) 134–144.
- [9] S. Chatterjee, D.S. Lee, M.W. Lee, S.H. Woo, Enhanced adsorption of congo red from aqueous solutions by chitosan hydrogel beads impregnated with cetyl trimethyl ammonium bromide, *Bioresour. Technol.*, 100 (2009) 2803–2809.
- [10] C. O'Neill, F.R. Hawkes, D.L. Hawkes, N.D. Lourenco, H.M. Pinheiro, W. Delee, Colour in textile effluents—sources, measurement, discharge consents and simulation: A review, *J. Chem. Technol. Biotechnol.*, 74 (1999) 1009–1018.
- [11] G.A. Adebisi, Z.Z. Chowdhury, P.A. Alaba, Equilibrium, kinetic, and thermodynamic studies of lead ion and zinc ion adsorption from aqueous solution onto activated carbon prepared from palm oil mill effluent, *J. Clean. Prod.*, 148 (2017) 958–968.
- [12] Z.Z. Chowdhury, N.M. Julkapli, M.A. Atieh, M.A.H.A. Saadi, W.A. Yehye, Application of graphitic bio-carbon using two level factorial design for microwave assisted carbonization, *BioRes.*, 11 (2016) 3637–3659.
- [13] G.A. Adebisi, Z.Z. Chowdhury, S.B.A. Hamid, E. Ali, Hydrothermally treated banana empty fruit bunch fiber activated carbon for Pb(II) and Zn(II) removal, *BioRes.*, 11 (2016) 9686–9709.
- [14] Z.Z. Chowdhury, S.B.A. Hamid, M.M. Rahman, R.F. Rafique, Catalytic activation and application of micro-spherical carbon derived from hydrothermal carbonization of lignocellulosic biomass: statistical analysis, *RSC Adv.*, 6 (2016) 102680–102694.
- [15] E. Khan, M. Li, C.P. Huang, Hazardous waste treatment technologies, *Water Environ. Res.*, 55 (2008) 1654–1708.
- [16] A. Tor, Y. Cengeloglu, Removal of congo red from aqueous solution by adsorption onto activated red mud, *J. Hazard. Mater.*, B138 (2006) 409–415.
- [17] J. Song, W. Zou, Y. Bian, F. Su, R. Han, Adsorption characteristics of methylene blue by peanut husk in batch and column modes, *Desalination*, 265 (2011) 119–125.
- [18] G. Crini, Non-conventional low cost adsorbents for dye removal: A review, *Bioresour. Technol.*, 97 (2006) 1061–1085.

- [19] M.T. Sulak, E. Demirbas, M. Kobya, Removal of astrazon yellow 7GL from aqueous solutions by adsorption onto wheat bran, *Bioresour. Technol.*, 98 (2007) 2590–2598.
- [20] V. Vadivelan, K. Vasanth Kumar, Equilibrium, kinetics, mechanism, and process design for the sorption of methylene blue onto rice husk, *J. Colloid Interface Sci.*, 286 (2005) 90–100.
- [21] M. Arami, N.Y. Limaee, N.M. Mahmoodi, N.S. Tabriz, Removal of dyes from colored textile wastewater by orange peel adsorbent: Equilibrium and kinetic studies, *J. Colloid Interface Sci.*, 288 (2005) 371–376.
- [22] B.H. Hameed, Evaluation of papaya seeds as a novel non-conventional low-cost adsorbent for removal of methylene blue, *J. Hazard. Mater.*, 162 (2009) 939–944.
- [23] K.G. Bhattacharyya, S. Arunima, *Azadirachta indica* leaf powder as an effective biosorbent for dyes: a case study with aqueous congo red solutions, *J. Environ. Manage.*, 71 (2004) 217–229.
- [24] B.H. Hameed, A.A. Ahmad, Batch adsorption of methylene blue from aqueous solution by garlic peel, an agricultural waste biomass, *J. Hazard. Mater.*, 164 (2009) 870–875.
- [25] V.K. Gupta, R. Jain, S. Varshney, Removal of reactofix golden yellow 3 RFN from aqueous solution using wheat husk—an agricultural waste, *J. Hazard. Mater.*, 142 (2007) 443–448.
- [26] A. Srinivasan, T. Viraraghavan, Decolorization of dye wastewaters by biosorbents: A review, *J. Environ. Manage.*, 91 (2010) 1915–1929.
- [27] Y. Fu, T. Viraraghavan, Fungal decolorization of dye wastewaters: A review, *Bioresour. Technol.*, 79 (2001) 251–262.
- [28] T. Akar, T.A. Demir, I. Kiran, A. Ozcan, A.S. Ozcan, S. Tunali, Biosorption potential of *Neurospora crassa* cells for decolorization of acid red 57 dye, *J. Chem. Technol. Biotechnol.*, 81 (2006) 1100–1106.
- [29] Y. Zeroual, B.S. Kim, C.S. Kim, M. Blaghen, K.M. Lee, A comparative study on biosorption characteristics of certain fungi for bromophenol blue dye, *Appl. Biochem. Biotechnol.*, 134 (2005) 51–60.
- [30] T. Akar, I. Tosun, Z. Kaynak, E. Kavas, G. Incirkus, S.T. Akar, Assessment of the biosorption characteristics of a macro-fungus for the decolorization of acid red 44 (AR44) dye, *J. Hazard. Mater.*, 171 (2009) 865–871.
- [31] Z. Aksu, F. Gonen, Biosorption of phenol by immobilized activated sludge in a continuous packed bed: prediction of breakthrough curves, *Process Biochem.*, 39 (2004) 599–613.
- [32] R. Sudha Bai, T.E. Abraham, Studies on chromium(VI) adsorption-desorption using immobilized fungal biomass, *Bioresour. Technol.*, 87 (2003) 17–26.
- [33] Z. Aksu, S.S. Cagatay, F. Gonen, Continuous fixed bed biosorption of reactive dyes by dried *Rhizopus arrhizus*: Determination of column capacity, *J. Hazard. Mater.*, 143 (2007) 362–371.
- [34] C.E. Borba, R. Guirardello, E.A. Silva, M.T. Veit, C.R.G. Tavares, Removal of nickel(II) ions from aqueous solution by biosorption in a fixed bed column: Experimental and theoretical breakthrough curves, *Biochem. Eng. J.*, 30 (2006) 184–191.
- [35] P.M. Doran, *Bioprocess engineering principles*, 2nd ed., Elsevier Science and Technology Publishing Company Limited, (2012).
- [36] P. Vairavel, V. Ramachandra Murty, S. Nethaji, Removal of congo red dye from aqueous solutions by adsorption onto a dual adsorbent (*Neurospora crassa* dead biomass and wheat bran): optimization, isotherm, and kinetics studies, *Desal. Water Treat.*, 68 (2017) 274–292.
- [37] A.A. Kadam, H.S. Lade, S.M. Patil, S.P. Govindwar, Low cost CaCl₂ pretreatment of sugarcane bagasse for enhancement of textile dyes adsorption and subsequent biodegradation of adsorbed dyes under solid state fermentation, *Bioresour. Technol.*, 132 (2013) 276–284.
- [38] I. Kiran, T. Akar, S. Tunali, Biosorption of Pb(II) and Cu(II) from aqueous solutions by pretreated biomass of *Neurospora crassa*, *Process Biochem.*, 40 (2005) 3550–3558.
- [39] M.C. Somasekhara Reddy, Removal of direct dye from aqueous solutions with an adsorbent made from tamarind fruit shell, an agricultural solid waste, *J. Sci. Ind. Res.*, 65 (2006) 443–446.
- [40] T.V.N. Padmesh, K. Vijayaraghavan, G. Sekaran, M. Velan, Biosorption of acid blue 15 using water macroalga *Azolla filiculoides*: Batch and column studies, *Dyes Pigm.*, 71 (2006) 77–82.
- [41] B. Preetha, T. Viruthagiri, Batch and continuous biosorption of chromium(VI) by *Rhizopus arrhizus*, *Sep. Purif. Technol.*, 57 (2007) 126–133.
- [42] S. Nethaji, A. Sivasamy, R. Vimal Kumar, A.B. Mandal, Preparation of char from lotus seed biomass and the exploration of its dye removal capacity through batch and column adsorption studies, *Environ. Sci. Pollut. Res.*, 20 (2013) 3670–3678.
- [43] W. McCabe, J. Smith, P. Harriott, *Unit operations of chemical engineering*, 5th ed., McGraw Hill Publishing Company Limited, (2004).
- [44] R. Han, J.H. Zhang, W.H. Zou, H.J. Xiao, J. Shi, H.M. Liu, Biosorption of copper(II) and lead(II) from aqueous solution by chaff in a fixed-bed column, *J. Hazard. Mater.*, B133 (2006) 262–268.
- [45] R. Han, Y. Wang, X. Zhao, Y. Wang, F. Xie, J. Cheng, M. Tang, Adsorption of methylene blue by phoenix tree leaf powder in a fixed-bed column: Experiments and prediction of breakthrough curves, *Desalination*, 245 (2009) 284–297.
- [46] E. Malkoc, Y. Nuhoglu, Y. Abali, Cr(VI) adsorption by waste acorn of *Quercus ithaburensis* in fixed beds: Prediction of breakthrough curves, *Chem. Eng. J.*, 119 (2006) 61–68.
- [47] E. Boyaci, A.E. Eroglu, T. Shahwan, Sorption of As(V) from waters using chitosan and chitosan-immobilized sodium silicate prior to atomic spectrometric determination, *Talanta*, 80 (2010) 1452–1460.
- [48] R. Aravindhhan, N.N. Fathima, J.R. Rao, B.U. Nair, Equilibrium and thermodynamic studies on the removal of basic black dye using calcium alginate beads, *Colloids Surf. A Physicochem. Eng. Asp.*, 299 (2007) 232–238.
- [49] Lunhong Ai, Ming Li, Long Li, Adsorption of methylene blue from aqueous solution with activated carbon/cobalt ferrite/alginate composite beads: Kinetics, isotherms, and thermodynamics, *J. Chem. Eng. Data*, 56 (2011) 3475–3483.
- [50] N. Rangsayatorn, P. Pokethitiyook, E.S. Upatham, G.R. Lanza, Cadmium biosorption by cells of *Spirulina platensis* TISTR 8217 immobilized in alginate and silica gel, *Environ. Int.*, 30 (2004) 57–63.
- [51] N. Saravanan, T. Kannadasan, C.A. Basha, V. Manivasagan, Biosorption of textile dye using immobilized Bacterial (*Pseudomonas aeruginosa*) and fungal (*Phanerochate chrysosporium*) cells, *Am. J. Environ. Sci.*, 9 (2013) 377–387.
- [52] A. Sivasamy, S. Nethaji, J.L. Nisha, Equilibrium, kinetic and thermodynamic studies on the biosorption of reactive acid dye on *Enteromorpha flexuosa* and *Gracilaria corticata*, *Environ. Sci. Pollut. Res.*, 19 (2012) 1687–1695.
- [53] ASTM International, *Annual book of ASTM standards, Water and Environmental Technology*, v. 11.01, West Conshohocken, Pennsylvania, (2003) 6–7.
- [54] APHA, *Standard methods for examination of water and wastewater*, 19th ed., American Public Health Association, Washington D.C., (1995).
- [55] APHA, *Standard methods for examination of water and wastewater*, 22nd ed., American Public Health Association, Washington D.C., (2012).
- [56] R.K. Trivedy, P.K. Goel, *Chemical and biological methods for water pollution studies*, Environmental Publication, India, (1986).
- [57] N.E. Messaoudi, M.E. Khomri, A. Dbik, S. Bentahar, A. Lacherai, B. Bakiz, Biosorption of congo red in a fixed-bed column from aqueous solution using jujube shell: Experimental and mathematical modeling, *J. Environ. Chem. Eng.*, 4 (2016) 3848–3855.
- [58] K. Vijayaraghavan, J. Jegan, K. Palanivelu, M. Velan, Removal of nickel(II) ions from aqueous solution using crab shell particles in a packed bed up-flow column, *J. Hazard. Mater.*, 111 (2004) 223–230.
- [59] A.A. Ahmad, B.H. Hameed, Fixed-bed adsorption of reactive azo dye onto granular activated carbon prepared from waste, *J. Hazard. Mater.*, 175 (2010) 298–303.

- [60] R. Han, Y. Wang, W. Zou, Y. Wang, J. Shi, Comparison of linear and nonlinear analysis in estimating the Thomas model parameters for methylene blue adsorption onto natural zeolite in fixed-bed column, *J. Hazard. Mater.*, 145 (2007) 331–335.
- [61] P.X. Sheng, K.H. Wee, Y.P. Ting, J.P. Chen, Biosorption of copper by immobilized marine algal biomass, *Chem. Eng. J.*, 136 (2008) 156–163.
- [62] V.K. Gupta, A. Mittal, L. Krishnan, V. Gajbe, Adsorption kinetics and column operations for the removal and recovery of malachite green from wastewater using bottom ash, *Sep. Purif. Technol.*, 40 (2004) 87–96.
- [63] K. Vijayaraghavan, M.W. Lee, Y.S. Yun, A new approach to study the decolorization of complex reactive dye bath effluent by biosorption technique, *Bioresour. Technol.*, 99 (2008) 5778–5785.
- [64] Metcalf, Eddy, *Wastewater engineering: Treatment and reuse*, 4th ed., Tata McGraw-Hill Publishing Company Limited, India, (2003).
- [65] R.O. Yusuff, J.A. Sonibare, Characterization of textile industries effluents in Kaduna, Nigeria and pollution implications, *Global Nest: the Int. J.*, 6 (2004) 212–221.